Development 122, 1313-1322 (1996)
Printed in Great Britain © The Company of Biologists Limited 1996
DEV4641

Characterizing the zebrafish organizer: microsurgical analysis at the early-shield stage

John Shih* and Scott E. Fraser

Division of Biology, Beckman Institute, California Institute of Technology, Pasadena, California 91125, USA

*Author for correspondence (e-mail: jshih@gg.caltech.edu)

SUMMARY

The appearance of the embryonic shield, a slight thickening at the leading edge of the blastoderm during the formation of the germ ring, is one of the first signs of dorsoventral polarity in the zebrafish embryo. It has been proposed that the shield plays a role in fish embryo patterning similar to that attributed to the amphibian dorsal lip. In a recent study, we fate mapped many of the cells in the region of the forming embryonic shield, and found that neural and mesodermal progenitors are intermingled (Shih, J. and Fraser, S. E. (1995) *Development* 121, 2755-2765), in contrast to the coherent region of mesodermal progenitors found at the amphibian dorsal lip. Here, we examine the fate and the inductive potential of the embryonic shield to determine if the intermingling reflects a different mode of embryonic patterning than that found in amphibians. Using the microsurgical techniques commonly used in amphibian and avian experimental embryology, we either grafted or deleted the region of the embryonic shield. Homotopic grafting experiments confirmed the fates of cells within the embryonic shield region, showing descendants in the hatching gland, head mesoderm, notochord, somitic mesoderm, endoderm and ventral aspect of the neuraxis. Heterotopic grafting experiments demonstrated that the embryonic shield can organize a second embryonic axis; however, contrary to our expectations based on amphibian research, the graft contributes extensively to the ectopic neuraxis. Microsurgical deletion of the embryonic shield region at the onset of germ ring formation has little effect on neural development: embryos with a well-formed and well-patterned neuraxis develop in the complete absence of notochord cells. While these results show that the embryonic shield is sufficient for ectopic axis formation, they also raise questions concerning the necessity of the shield region for neural induction and embryonic patterning after the formation of the germ ring.

Key words: zebrafish, induction, shield, microsurgery, homology, organizer, dorsal lip, gastrulation

INTRODUCTION

Gastrulation in the zebrafish embryo begins with the process of epiboly, during which the blastoderm spreads to cover the large yolk mass. Around the time when the blastoderm margin reaches the equator (termed 50% epiboly; Westerfield, 1994; Kimmel et al., 1995), cells move inward from the primary ectodermal layers of deep cells along the blastoderm margin and coalesce to form an inner layer, the primitive hypoblast. This inward movement forms the bi-laminar germ ring. As the primitive hypoblast forms, the embryonic shield appears as a greater local thickening along the blastoderm margin; this serves as the first clear manifestation of the future dorsal side of the embryo. Zebrafish development has been described as closely resembling that of amphibians (Kimmel et al., 1990; Warga and Kimmel, 1990) and, by analogy, the embryonic shield of teleostean fishes has been proposed to function as an 'organizer' resembling the dorsal lip of the blastopore in amphibians. Microsurgical grafting experiments, in which the embryonic shield is transplanted ectopically in *Fundulus* and *Perca* (Oppenheimer, 1936b), and trout (Luther, 1935), has demonstrated that the shield can induce the formation of an ectopic embryonic axis, composed apparently of both graft and host cells. Some of the key signals underlying the shield's inductive capacity appear to be shared between species; for example, implantation of half of a zebrafish blastoderm into a *Triturus torosus* blastocoel can induce the formation of an ectopic axis in the host (Oppenheimer, 1936a). More recent transplantations, using a micropipette to transfer a small number of cells from the dorsal germ ring into the ventral germ ring in the zebrafish embryo, have confirmed the inductive capacity of cells in the embryonic shield (see review: Ho, 1992), although the distributions and fates of the transplanted cells were not noted.

Recently, we fate mapped the outer three layers of deep cells of the zebrafish embryonic shield region (at the early-shield stage, just as the germ ring begins to take shape; Shih and Fraser, 1995) by carefully documenting the positions of the single cells that were iontophoretically labeled with fluorescent dextran. This fate map demonstrates that the progenitor cells of the neurectodermal and the chordamesodermal lineages are intermingled in the shield region. This arrangement differs from the presumptive tissue distributions in the amphibian

embryo, where neurectodermal and chordamesodermal lineages occupy distinct and separate domains at the onset of gastrulation (Keller, 1975, 1976; Vogt, 1929). It is unclear whether this difference in progenitor topography between the zebrafish and the amphibians reflects differences in the timing and geometry of neural induction. As the intermingled progenitor distribution of the zebrafish shield may be a common feature of many vertebrate embryos (see Shih and Fraser, 1995, and Discussion), an examination of the inductive interactions underlying neural development in the zebrafish could yield insights into the mechanism of vertebrate neurogenesis.

Here, we present the second in a series of experiments directed towards developing a better characterization of the inductive interactions within, and the differentiative properties of, the zebrafish embryonic shield. We have adopted the microsurgical techniques used by Oppenheimer in her analysis of tissue interactions during *Fundulus* gastrulation (Oppenheimer, 1936b) in order to explore the timing and mechanism of zebrafish neural induction. Microsurgical manipulation, which allows the orientation and position of the grafted tissues to be carefully controlled, is ideally suited for exploring tissue interactions in vertebrate development. Much of our knowledge of the tissue interactions that are important for amphibian and avian development was gained by applying these microsurgical grafting techniques. Alternate technologies that use a micropipette to transplant a single or a small number of cells are best suited for studying questions of cell fate determination (Ho and Kimmel, 1993). In our first experiment, we homotopically replaced the early shield with one from a labeled donor and confirmed the tissue progenitor distribution in the shield region reported previously (Shih and Fraser, 1995). Second, we transplanted an early shield from a labeled donor into the ventral germ ring of an unlabeled sibling host. The formation of ectopic axes confirm the 'organizer-like' properties of the zebrafish embryonic shield; however, the distributions of graft-derived and host-derived progeny in the ectopic axes are different from those observed in amphibians (Smith and Slack, 1983). Last, we tested whether the shield is necessary for embryonic development. Surprisingly, we found that shield deletion at the early-shield stage can result in the formation of a notochordless embryo in which the nervous system and somitic mesoderm appear well patterned. These observations are consistent with the suggestion, raised by our previous fate-mapping experiments, that neural induction may be well underway by the onset of germ ring formation.

MATERIALS AND METHODS

Embryo collection

General maintenance, embryo collection and staging of the zebrafish (*Danio rerio*) were carried out according to the *Zebrafish* book (Westerfield, 1994). The embryos were kept at 28.5°C in 30% Danieau solution (full-strength Danieau is the same as amphibian Modified Niu-Twitty solution (Keller, 1991) with double the normal $CaCl_2$ concentration), except during microsurgical manipulation, for which we used full-strength Danieau solution. During and after surgery, all embryos were kept at room temperature and staged according to the morphological criteria provided in the *Zebrafish* book.

Embryo labeling and microsurgery

Donor embryos were labeled by pressure injecting 2 nl of fluorescein dextran (100 mg per ml dissolved in sterilized water; 10,000 M_r anionic, lysine fixable, cat# D-1820; or 3,000 M_r anionic, lysine fixable, cat# D-3306, Molecular Probes) into 4-cell-stage embryos when the cells were still syncytial. Surgery was performed in full-strength Danieau solution in either 60 mm Falcon tissue culture dishes (cat#3002, Becton Dickinson) or in Pyrex glass dishes. An eyelash-hair knife and a hairloop were used for surgical manipulations, (See Keller, 1991, for surgical technique, tools and basic solution recipe.) Micromanipulation of the embryonic shield was done at the early-shield stage (as defined in Shih and Fraser, 1995). The experiments described in this paper are diagrammatically illustrated in Fig. 1.

We present paired data from 240 organizer-graft and shield-deletion experiments. In each pair, the shield was excised from a labeled embryo and implanted into the ventral germ ring of a sibling host (Fig. 1). Raising the embryos as pairs allowed the results to be cross-checked. The host was scored as an organizer-graft experiment and the donor was scored as a deletion. An additional 20 deletion embryos (unlabeled) were used for antibody staining; these were not done as a part of any set and are reported separately.

Documentation

The embryos were mildly anesthetized in 30% Danieau with Finquel (100 mg/liter, tricaine methanesulfonate, Argent Chemical Labs) and then transferred to a Sylgard-based plate (Sylgard 182 silicone elastomer, Dow Corning, cured and then pretreated with 2% BSA solution) with precut triangular wells, filled with 30% Danieau with Finquel solution. The positions, distributions and fates of labeled graft progeny were monitored and documented in the living whole-mount using a SIT camera (Hamamatsu C2400) mounted on a Zeiss AxioPhot microscope. Cell types were scored by the criteria previously established in Shih and Fraser (1995). Low-magnification and epi-illuminated images were taken on a Zeiss Stemi SV-11 fitted with a Hitachi KP-C5010 color camera. Bright-field transmitted images were taken on a Zeiss AxioPhot using a Hamamatsu Neuvicon camera. In each case, the images were captured on a 151 image processor (Imaging Technologies, Inc.) and averaged (n=8 frames) before storage on optical memory disk (Panasonic OMDR 3038) using the VIDIM image-processing software (authored by Belford, Fraser and Stollberg). After imaging, the embryos were collected, fixed with 4% formaldehyde in 0.1M PBS pH 6.9 containing 2.5% DMSO and processed for histology. Paraplast sections were cut at 10 μm.

Antibody staining

Shield-deletion embryos were fixed in MEMFA for 30-45 minutes and processed in a manner similar to the published protocol for *Xenopus* (Klymkowsky and Hanken, 1991). They were rinsed in doubly distilled water, pipetted into –20°C methanol and kept overnight in the freezer. After equilibration to room temperature, the embryos were transferred through graded MEOH/PBS series into PBS. Non-specific staining was blocked using 2% BSA in PBS for 30 minutes. Embryos were then transferred to primary antibody solution (1/1000 dilution of Tor-70 ascites stock with 2% BSA solution in PBS; Tor-70 was a gift from Dr P. Kushner) and incubated at 4°C overnight. The embryos were then washed extensively over a 6 hour period and placed into secondary antibody solution (Goat anti-mouse peroxidase-conjugated 1/500, Cappel) for overnight incubation at 4°C. Staining was visualized in 1 ml of 0.25 mg/ml diaminobenzidine (Sigma) with 5 μl of 1 N NiCl and 5 μl of 10% hydrogen peroxide.

RESULTS

Homotopic shield grafts

We homotopically replaced the embryonic shield region at the early-shield stage with one from a sibling donor labeled with

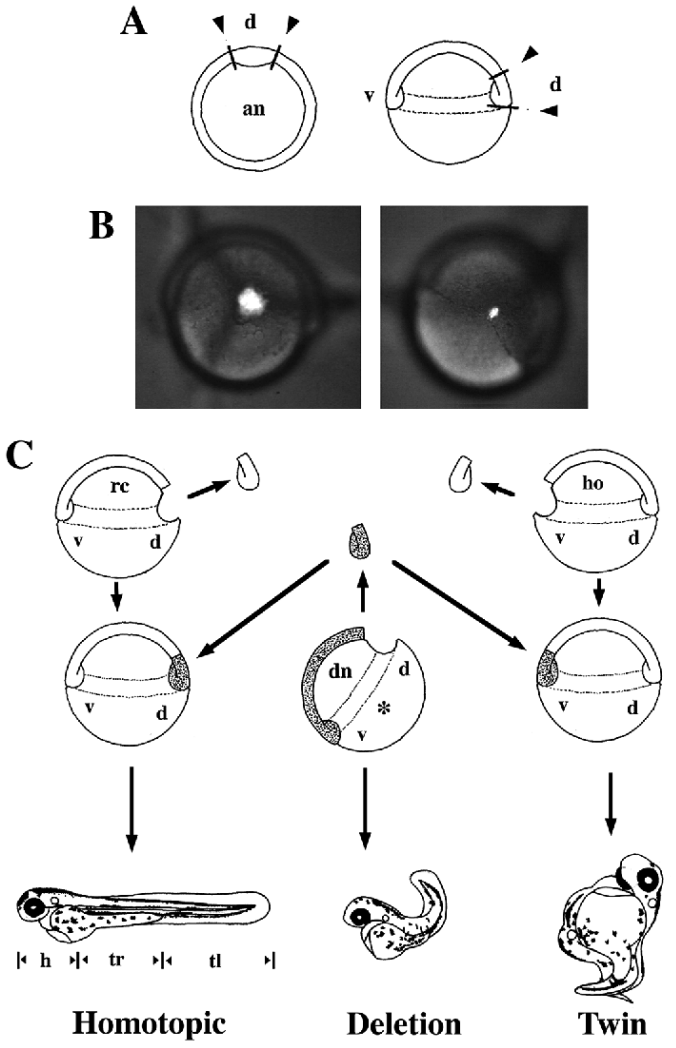

Fig. 1. Schematic of the experimental manipulations. (A) Position and size of the embryonic shield as it first becomes visible around 50% epiboly. It is roughly 20 cells wide (along the blastoderm margin), 12 cells tall (from the blastoderm margin) and 6-8 cells thick. [Left: animal-pole view; right: profile view.] The arrows and dark bars show the position of cuts made to excise the shield region; this included both the primary epiblast and the primitive hypoblast (full thickness of the shield). The dotted lines represent the germ ring along the equator of the embryo. (B left) An embryo in which the whole of the early-shield region is homotopically replaced with one from a fluorescein-dextran-labeled donor, viewed and imaged using low-light-level epifluorescence microscopy just after healing. (See Fig. 2A for progeny distribution.) The images shown in the Figures are not photocomposite. (B right) Homotopic replacement of 15-30 cells centered at the midline of the shield region. (See Fig. 2B for progeny distribution.) (C) Schematic diagrams of the early shield transplantation, replacement and deletion operations. (Left) To fate map the early shield, early shields were excised from a fluorescein-dextran-labeled donor embryo (dn) and implanted into the same position of an unlabeled sibling recipient (rc). The donors were retained and used as shield-deletion animals. (Right) Twinned embryos were made by implanting labeled shields from donor embryos (dn, shaded) into the ventral germ rings of unlabeled sibling hosts (ho). The position of the labeled cells along the length of the axis were specified as being in the head region (h), including the forebrain, midbrain and hindbrain; the trunk (tr), from the rostral end of the spinal cord to the level of the anus; and the tail (tl), caudal to the anus. Abbreviations: an, animal pole; d, dorsal side; dn, donor; h, head region; ho, host embryo; rc, recipient embryo; tl, tail region; tr, trunk region; v, ventral side.

fluorescent dextran (*n*=68; see Fig. 1B, left and 1C, left); the graft healed rapidly. The distribution of labeled progeny is in agreement with expectations based on the general fate map of the early gastrula (Kimmel et al. 1990) and the detailed fate map of the embryonic shield region (Shih and Fraser 1995). Labeled progeny arising from the early shield contributed to hatching gland, rostral endoderm, head mesoderm, notochord, a limited amount of somitic mesoderm and some ventral neural tissues (Fig. 2A,E). Floorplate cells, identified by their unmistakable morphology and position at the ventral midline of the neural tube, were also among the early-shield derivatives (Fig. 2). Both the notochord and floorplate were solidly labeled from the axial level of the ear to the level of the anus. The ventral aspect of the midbrain and hindbrain contained labeled progeny appearing as bilaterally symmetrical clusters of neurons (Fig. 2E, shows such paired neural clusters in the caudal hindbrain.) Caudal to the anus, in the tail region, both the neural tube and axial mesoderm were intermittently labeled in the majority of cases (Fig. 2A). Sometimes, solid labeling of these structures extended farther into the tail (21/68=31%, Fig. 2C), although in no case was either the tail notochord or floorplate wholly labeled. More superficially, labeled cells were observed in the overlying periderm, along the dorsal-most portion of the fin over the trunk region (Fig. 2A,C) and, very occasionally, in the dorsal neural tube (2/68=3%, in the caudal trunk to tail, Fig. 2G).

We confirmed the intermingled-neighbor relationship of different tissue progenitors reported in our previous fate-mapping experiments (Shih and Fraser, 1995) by making smaller grafts, contained entirely within the visible outlines of the embryonic shield. If the tissue progenitors are intermingled neighbors in the embryonic shield region, then smaller grafts should also give rise to the same range of tissue progeny described in the preceding section. We made small homotopic grafts at the dorsal midline that spanned the full thickness of the shield region (6-8 cells thick) and encompassed roughly 15-30 cells (Fig. 1B right, *n*=60). These gave rise to labeled descendants in the same tissue types observed when the entire shield region was replaced (Fig. 2B).

Heterotopic shield grafts

To test the ability of the embryonic shield to induce an ectopic axis, we grafted a labeled embryonic shield at the early-shield stage into the germ ring at the ventral midline of an unlabeled sibling host after excising a same-sized region from the ventral germ-ring (*n*=240, Fig. 1C right-side diagram). The graft healed in place within 15 minutes, by which time its borders were no longer obvious. Both donor and recipient embryos completed epiboly at the same time as controls. Examination under a dissecting microscope clearly indicated that the early shield possesses inductive potential, in that an ectopic axis formed in response to the shield transplant. Sham replacements of either the ventral (*n*=16, Fig. 3C) or the dorsal (*n*=10) germ ring, as well as the excision of the ventral germ ring alone (*n*=12, 5C middle), all produced embryos indistinguishable from controls.

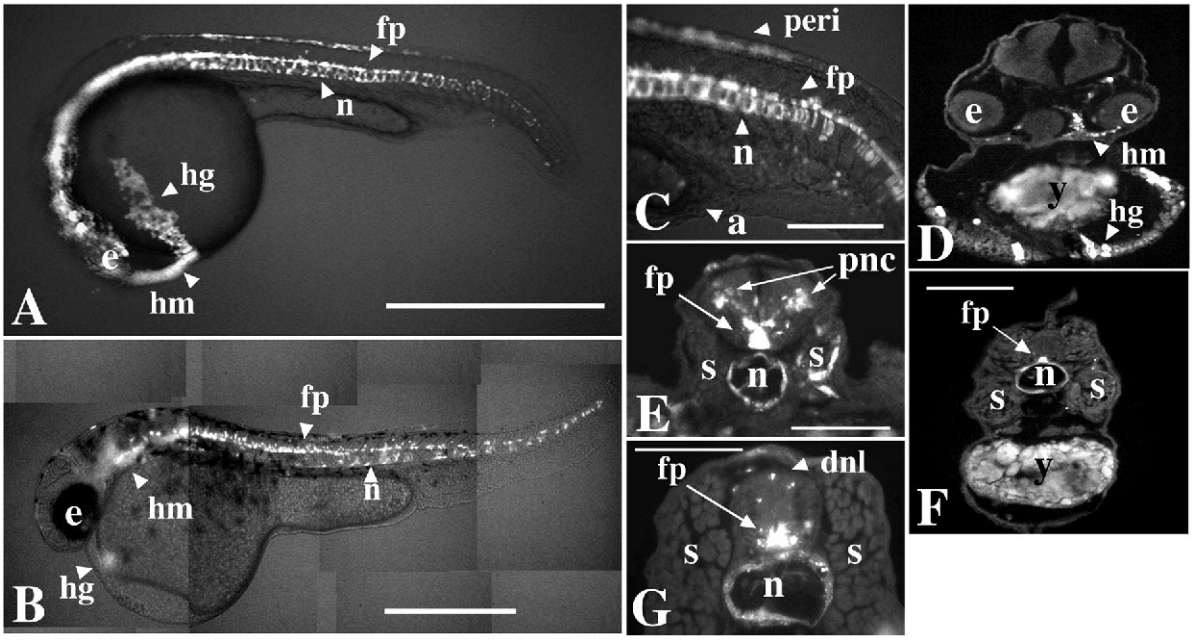

Fig. 2. Fate mapping the embryonic shield. Embryos in which the early shield was replaced with one from a fluorescein-dextran-labeled donor were scored at 24-36 hours in the whole mount and in histological sections. (A) In the whole mount, the labeled descendants were clearly in the notochord (n), head mesoderm (hm), hatching gland (hg), floorplate (fp) and the dorsal fin. (B) Smaller grafts of around 30 cells, centered at the dorsal midline and encompassing the full depth of the blastoderm, and contained completely within the outlines of the shield, contributed to the same tissue types that were observed when the entire shield region was replaced with labeled tissue. Labeled progeny spanned the full length of the axis, from the hatching gland (hg arrow) to the tip of the tail. (C) In higher magnification, it is clear in the tail region that the notochord and the floorplate, rostral to at least the level of the anus (a), were entirely derived from the labeled shield. Unlabeled recipient cells also contributed to these structures caudal to the anus (a). In this example (representing 31% of total), solid labeling of the notochord and floorplate extended farther into the tail and appears to have made a greater contribution to the floorplate (fp) than to the notochord (n) in the tail. (D) In sections at the level of the eyes, labeled shield derivatives were found in the hatching gland (hg) and head mesoderm (hm). (E) In the rostral spinal cord and the caudal hindbrain regions, the graft cells formed the notochord (n), floorplate (fp) and paired neuron clusters (pnc), and contributed to the overlying enveloping layer. Labeled cells were also present in the somitic mesoderm (s). (F) The only two structures consistently labeled in the trunk were the notochord and floorplate. (G) In 2/68 embryos, there were scattered labeled cells in the dorsal portion of the neural tube (dnl); given their size and location, they may be neural crest, although their identity is not known for certain. Abbreviations: a, anus; dnl, dorsal neural label; e, eye; fp, floorplate; hg, hatching gland; hm, head mesoderm; n, notochord; nt, neural tube; peri, periderm; pnc, paired neural clusters; s, somitic mesoderm; y, yolk. Scale bar: A,B, 500 μm; C-F, 50 μm. Stages A,C 24 hours; B, D-F 36 hours.

The distribution of labeled cells was assessed and documented in living whole mounts using low-light-level microscopy, after which the embryos were processed histologically for further analyses. Under epifluorescence, it was clear that, in the majority of living whole-mounts, the early shield transplants induced a second, distinct embryonic axis composed of both host- and graft-derived cells (178/240=74%, Figs 3A,B, 4A-E). These embryos were shorter than the controls. The host and ectopic axes were separated by less than 45 degrees at 24 hours of development (Figs 3A,B, 4A-E). Periodic examination in the dissecting microscope using epifluorescence showed that the labeled graft cells coalesced during epiboly into an axial array near the ventral midline. Shortly after yolk-plug closure, the ectopic axis began moving towards the host axis. None of the ectopic axes had eyes or any other obvious forebrain or midbrain structures. The full length of the notochord in the ectopic axis was graft-derived as was much of the ectopic neural tube. The length of the notochord varied considerably and there appears to be an inverse relationship between the length of the ectopic notochord and the degree to which the graft contributes to the ectopic neuraxis. Ectopic heart formation was observed rarely (3/240=1%); in each case, the heart tissue was of host origin.

In histological sections, partial duplication of the rostral neuraxis was clear, even in twinned embryos where the axes were closely apposed (Fig. 4A,B). Much of the ectopic hindbrain, the ventral aspect of the ectopic spinal cord and all of the ectopic notochord were graft-derived (Fig. 4A-D). Caudally, the host and the ectopic neural tubes merged into a single structure that appears to be ‘anchored’ to each notochord by a floorplate (Fig. 4D). Somites in the ectopic axes were host derived (some scattered labeled cells were occasionally noted in the somites, although none had somite cell morphology). These somites were asymmetrically distributed around the paired notochords such that the greater mass of somitic tissue was between the two notochords and under the neural axis (Fig. 4E). In those twinned embryos in which the ectopic notochord approached normal length and the paired notochords were separated by somitic mesoderm, the merged neuraxis in the caudal trunk and tail region was encircled by segmented somitic tissue (31/240=13%, Fig. 4E).

In a small minority of twins, the host and ectopic axes

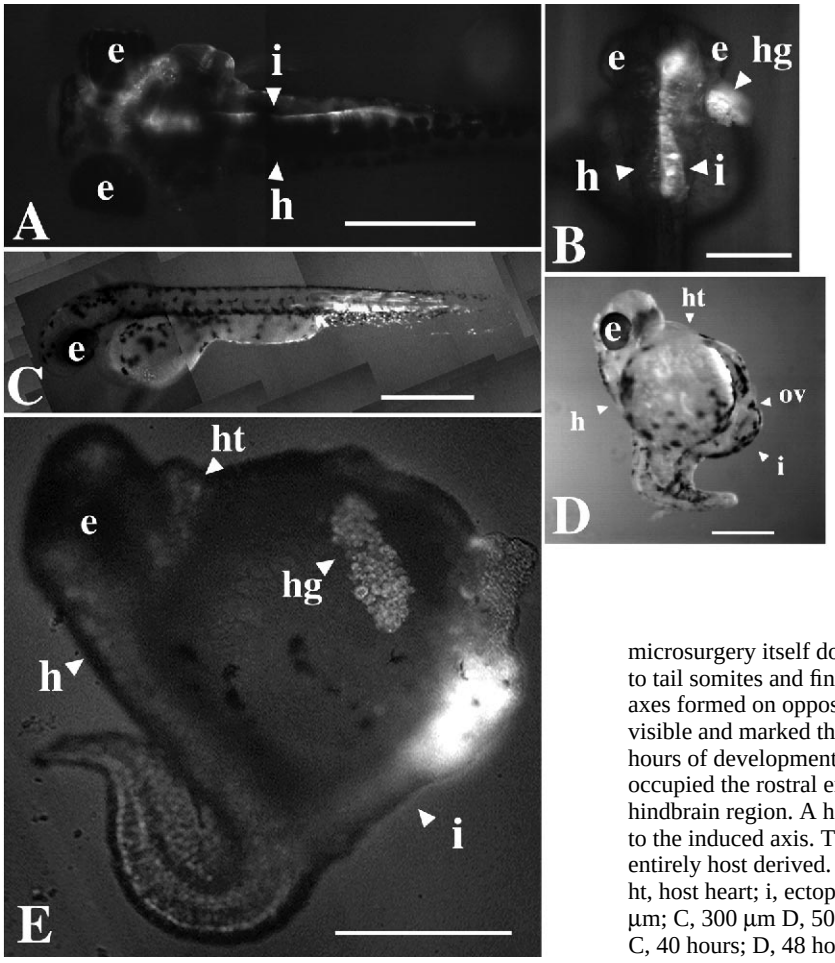

Fig. 3. Heterotopic shield grafts. Grafting the early shield from embryos at 50% epiboly into the ventral germ ring of sibling hosts resulted in the formation of ectopic axes. (A) In the majority of cases, the presence of the ectopic axis (i) was not always obvious, as it sometimes paralleled that of the host (h). In the example shown in A and B, the embryos did not appear to be twinned when examined using a dissecting microscope; however, if viewed using epifluorescence, the presence of the ectopic notochord on one side of the midline was evident. Labeled cells were present in the hatching gland. The examples shown in A and B also illustrate the range in variation of the length of the ectopic axis from long (A) to short (B); in no case did the ectopic notochord extend to the level of the anus. (C) Homotopic replacement of the ventral germ ring yielded normal embryos; this showed that microsurgery itself does not cause axis duplication. Labeled cells contributed to tail somites and fin ectoderm. (D) In a minority of twinned embryos, the axes formed on opposite sides of the yolk. Otic vesicles (ov) were clearly visible and marked the position of the hindbrain in the ectopic axis. (E) At 24 hours of development, epifluorescence images show that graft-derived cells occupied the rostral end of the axis, appearing to be concentrated in the hindbrain region. A hatching gland (hg) was on the surface of the yolk lateral to the induced axis. The rostral-most neural tube appeared to be almost entirely host derived. Abbreviations: e, eye; h, host axis; hg, hatching gland; ht, host heart; i, ectopic axis; ov, otic vesicle. Scale bar: A, 200 μm; B, 500 μm; C, 300 μm D, 500 μm and E, 500 μm. Stages A, 72 hours; B, 36 hours; C, 40 hours; D, 48 hours; E, 36 hours.

remained on opposite sides of the yolk mass (5/178= 2%) (Fig. 3D,E). When viewed as living whole mounts, these '180 degree' twins displayed a graft-derived hatching gland, rostral and lateral to the rostral end of the ectopic neural axis, and within the surface ectoderm (Fig. 3E). In histological sections, the rostral-most end of the ectopic neural tube was entirely host derived and was underlain by a thin layer of graft-derived mesoderm (Fig. 4F). In the hindbrain region, at the level of the otic vesicles, the ectopic neural tube did not have the characteristic rhomboid shape but was smaller, appearing more like a normal spinal cord in cross section; close to half of this ectopic hindbrain was graft-derived (Fig. 4H). A discontinuous notochord, appearing to have broken into segments, first appears at the level of the hindbrain. This notochord extended only as far caudad as the rostral end of the spinal cord. The overlying neural tube was tilted with its lateral wall against the yolk mass (Fig. 4I), resembling the 'hemi-embryos' reported by Oppenheimer (1936b; in that paper, see figures 6, 8, 18 and 24). Labeled cells were observed in the ectopic neuraxis, extending for some distance into the spinal cord (Fig. 4J). At these caudal levels, the nerve cord appeared as a solid rod composed in part of graft-derived cells. In sections, host-derived somitic mesoderm cells were present in very small numbers, symmetrically distributed on both sides of the ectopic neuraxis (Fig. 4J).

A minority of the embryos (62/240=26%) receiving heterotopic shield grafts had two notochords but only a single neural tube (Fig. 4K-M). Even though an ectopic notochord was clearly present and had affected the development of the neuraxis, no distinct ectopic neuraxis was formed in response to the graft. Approximately half of these (32/62) had two host-derived floorplates and no graft contribution to the neural tube (Fig. 4K). In the remainder (30/62), the neural tube had only a single floorplate, despite the presence of two notochords in direct apposition with the ventral neural tube at the time of fixation. In such cases, the single floorplate ranged from mostly host derived to mostly graft derived (Fig. 4L).

Deletion of the early shield

Deletion of the embryonic shields at the early-shield stage produced embryos that were, in general, shorter and somewhat wider than controls, and that arched dorsalwards (n=240; see Fig. 1C, middle). In every case, they appeared rostrocaudally and dorsoventrally patterned (Fig. 5A,B). They formed eyes, forebrains, midbrains, hindbrains, spinal cords and segmented somites (Fig. 5A). Rostral to the hindbrain, the neural tube appeared somewhat smaller in diameter. In particular, the ventral portion of the diencephalon between the eyes appeared reduced in size and some embryos were cyclopic (86/240=36%; Fig. 5B, middle). In histological sections, otic vesicles and eye(s) were positioned more ventrally as compared to controls. A morphologically distinct floorplate

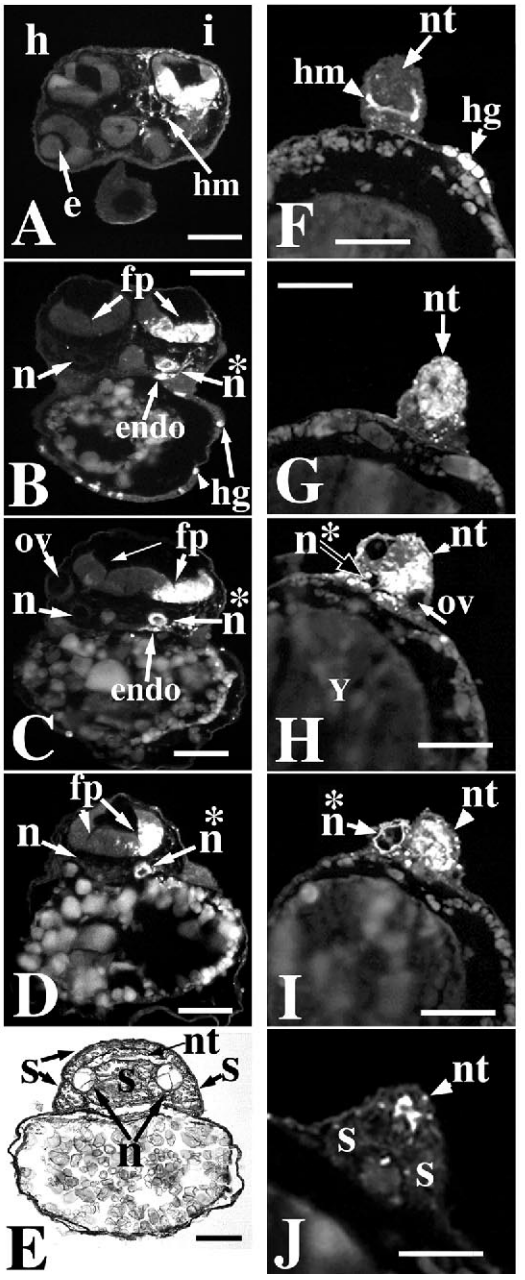

Fig. 4. Histological sections through the ectopic axes. Sections of a majority-case embryo in which the host and ectopic axes were closely apposed in parallel, starting with the eye level and ending with the caudal hindbrain level. The hindbrain was duplicated. Duplication of more-rostral neural structures was incomplete, as eye(s) were never observed (0/240) in the ectopic axis. Labeled graft cells gave rise to the entire ectopic notochord (n*) and ectopic rostral floorplate. (Ventral midline thinning was not observed in the caudal trunk and tail where the ectopic notochord was absent.) A large portion of the ectopic hindbrain was derived from the labeled graft tissue. In addition, roughly a third of the hatching gland cells were graft-derived (hg, intermixed with the host's hatching-gland cells), as were some of the endoderm (endo) and head mesoderm cells (hm). (E, section from an animal not a part of the A-D series) Somitic mesoderm in the more-caudal regions of the twinned embryos was distributed asymmetrically. The greater portion of the somitic mesoderm was always in the region between the paired notochords. In the example shown here, the ectopic notochord approached normal length and the neural tube has become a sheet of cells that appears as a 'bridge' between the paired notochords. The ectopic floorplate in such sections is graft-derived. Somitic mesoderm appears to enclose the neural axis, as somitic mesoderm both overlies and underlies the neural tissues. (F-J, 48 hours) Sections of the ectopic axis in '180 degree twins' revealed that the rostral-most neural tube (nt) of the ectopic axis was relatively featureless and was almost entirely host-derived (F). This neural tube was underlain by graft-derived head mesoderm (hm). To one side of this unlabeled portion of the ectopic neuraxis, within the surface ectoderm, there were graft-derived hatching-gland cells (hg). (G) Farther caudally, the rostral end of the hindbrain was almost entirely graft derived. (H) At the level of the otic vesicles (ov), half of the neural tube was graft derived and a small bit of notochord (n*, discernible as a small vacuole) was present beneath the neural tube. The hindbrain did not have its characteristic rhomboid appearance. (I) Caudal to the otoliths, near the rostral end of the spinal cord, the graft-derived notochord (n*) was lateral to the neural tube, on the surface of the yolk mass and was not flanked by somitic mesoderm. (J) At mid-trunk, the notochord was no longer present. Here, the neural tube was in part graft derived and was flanked bilaterally by host-derived somitic mesoderm. (K-L) In a minority of the embryos, only a single neural tube formed that was underlain by two notochords (one host derived, n, and the other graft derived, n*). In some cases, there were two floorplates, both host derived (K, hindbrain level); in the remainder, there was only a single floorplate (L). Abbreviations: e, eye; fp, floorplate; h, host axis; hg, hatching gland; hm, head mesoderm; i, ectopic axis; n, host notochord; n*, ectopic notochord; nt, neural tube; ov, otic vesicle; s, somitic mesoderm; y, yolk. Scale bars: 50 μm. Stages A-K, 48 hours; L, 60 hours.

was observed in the hindbrain, although it appeared to be missing in the trunk region. The majority of the embryos displayed an extensive, though not complete, absence of the shield's normal mesodermal derivatives (174/240=73%). Microscopic examination of this majority case in the live whole mount revealed the loss of all but a few hatching gland cells (5-10; Fig. 5A), and the loss of the notochord in the head and trunk. The remaining 66 (of 240; 27%) embryos did not appear to have either hatching gland cells or notochord cells in the axis. Further examination of these notochordless animals in histological sections confirmed the absence of notochord cells in the hindbrain and rostral trunk regions in all but four cases. These four had a single or few notochord cells ventral to the neuraxis; 44 of 66 cases had notochord cells in the caudal trunk and/or tail; 18 of 66 cases had no vacuolated cells throughout the entire length of the axis (from head to the tip of the tail). Somitic mesoderm formed bilateral files that were fused medially under the neural tube when the notochord was absent (Fig. 6K). Although still segmented, the somitic mesoderm formed rostrocaudally compressed rectangles instead of the characteristic 'chevrons' (Fig. 5A).

To complement the morphological analyses and to confirm the absence of notochord cells, we stained shield-deletion embryos for the presence of notochord cells at 15 hours of development, using the Tor-70 antibody (20 embryos from a separate set of deletion experiments, not included in the above 240). At 15 hours, the Tor-70 antibody labeled only the notochord, floorplate and the otoliths in control embryos (Fig. 6A-C, J). In the majority of deletions, there were a few well-vacuolated notochord cells in the axis (17/20=85%). These notochord cells were most frequently found in the tail region, although they were sometimes seen in the caudal trunk; 3 of

the 17 had either a single or a small cluster of 2-3 antibody-labeled cells in the rostral trunk/hindbrain (Fig. 6G,H,F). Floorplate-like staining was observed along the length of the axis, even in embryos where only a few notochord cells were present. In 3 of 20 (15%) cases, there was no notochord cell staining along the entire axis, indicating the complete absence of notochord cells from head to tail (Fig. 6D,E,K). Even in these more extreme examples, developing eye rudiments were present and clearly visible (Fig. 6I), and Tor-70 antibody labeling that was characteristic of the floorplate in control embryos was observed (Fig. 6K). This floorplate-like labeling was discontinuous, forming patches ranging from 20 to 80 μm in length, separated by gaps averaging around 20 micrometers (Fig. 6D,E,G,H). Bilateral otoliths were present and stained in all embryos, providing an internal positive control for the antibody procedures.

DISCUSSION

In this study, we have used microsurgical manipulations to better characterize the normal fate composition and inductive capacity of the zebrafish embryonic shield region. By homotopically replacing the shield region of a host embryo with one from a fluorescent-dextran-labeled donor, we were able to confirm and extend our previous fate map, which showed an intermingling of tissue progenitors within the shield region of the zebrafish early gastrula (Shih and Fraser, 1995). The labeled replacement shield contributed to most of the notochord, some somite cells, cells in the ventral neuraxis, including most of the floorplate, some endoderm, some head mesoderm cells and most of the hatching gland. We show that the same mixed set of descendants was obtained by transplanting small grafts of only 15-30 cells, centered at the midline and contained entirely within the outlines of the embryonic shield. Because these observations were consistent with expectations based upon the general fate map of the early gastrula (Kimmel et al. 1990) and the detailed fate map of the embryonic shield region (Shih and Fraser 1995), they demonstrate that microsurgery alone does not alter the prospective cell-fate composition of the embryonic shield. Moreover, they show that cell movements in the shield region seem unaltered by microsurgery, as the labeled progeny were dispersed by normal convergence and extension movements along the length of the axis.

The inductive properties of the amphibian dorsal lip was first demonstrated by transplanting a small circular piece of the dorsal lip from an unpigmented *Triton cristatus* embryo into the presumptive ectoderm of a pigmented *Triton taeniatus* embryo (Spemann and Mangold, 1924). In the days following the transplantation, an ectopic axis arose that was composed of both host and graft cells. The tissue contribution made by the graft to the ectopic axis varied from one experiment to the next. When the piece of upper blastoporal lip was taken from the beginning of gastrulation, it contributed to endoderm and mesoderm, whereas a piece taken from the upper lip of an 'advanced' gastrula contributed to neural tissues as well (Spemann and Mangold, 1924). The inductive influences of the advanced dorsal lip grafts was thought to originate from its mesodermal component. Bautzmann (1926; and see Spemann, 1938) mapped the spatial limit of the amphibian 'center of organization' in terms of its inductive influence and found it to coincide with the presumptive dorsal meso-endoderm domain; the activity was localized within the 'boundaries of invagination' as described by Vogt (1929). From the time of those first experiments, researchers have identified similar 'centers of organization' in other embryos and microsurgical transplantation experiments have shown that the Hensen's node in chicken

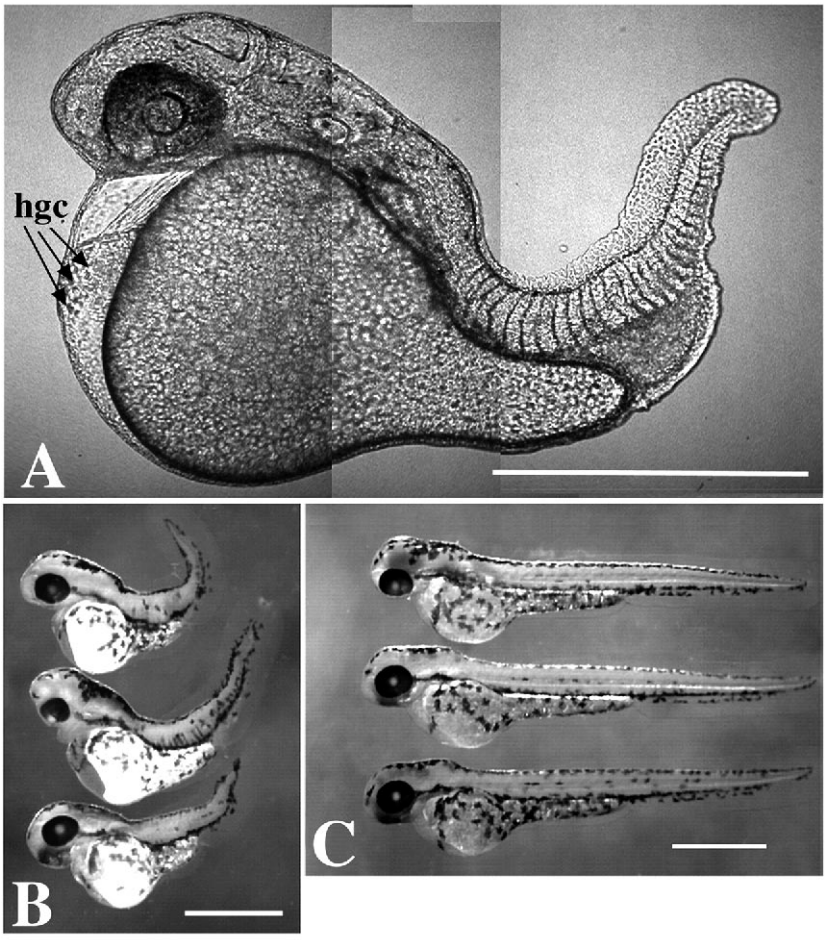

Fig. 5. Deletion of the embryonic shield. (A,B) After surgical deletion of the early shield at 50% epiboly, the embryos had remarkably complete neural axes. They formed rostral neural structures such as eyes; all the basic subdivisions of the brain were clearly visible. The somites formed rectangular blocks instead of the characteristic 'chevrons' (A). Roughly 30% of these were cyclopic (middle animal in B) and all were curved dorsalward. (C) Controls for ventral germ-ring deletion (top) and ventral germ-ring excision and replacement (middle) were indistinguishable from controls (bottom). Abbreviations: hgc, hatching gland cells (scored by distinct morphology; see figure 32 in Kimmel et al., 1995). Scale bars: 500 μm. Stages A, 30 hours; B, 48 hours; C, 48 hours.

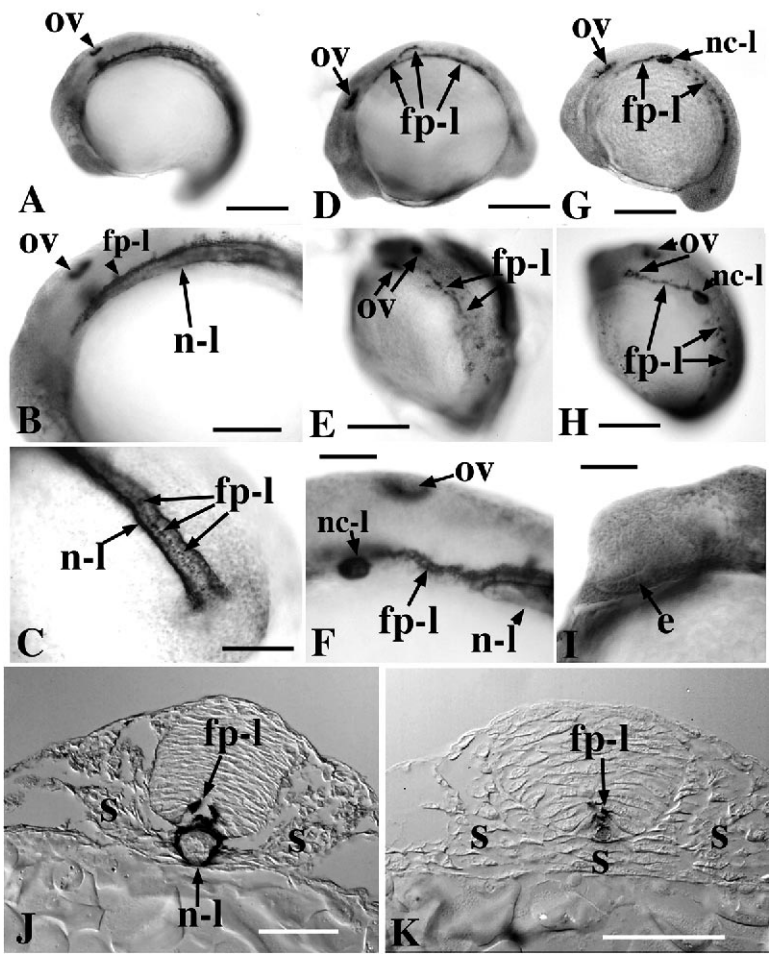

Fig. 6. Tor-70 labeling of shield-deletion embryos. (A-C) Control staining with the Tor-70 antibody at 15 hours of development labels only the notochord, floorplate and otolithes. (B) Under higher magnification, the staining pattern of the notochord can be clearly distinguished from that of the floorplate. The floorplate labeling (fp-l) ends a short distance rostral to the notochord (n-l) in the hindbrain. (C) In the tail region, the same tissues are labeled by the antibody, although not to the tip of the tail bud. (D,E,G,H) Two examples of the deletion embryos are shown. (D, E) The notochord was completely missing as there was no staining of vacuolated cells. (G,H) Another embryo shows that even when only two well-vacuolated notochord cells (n-l) are present, their staining is unmistakable. The only notochord cells are those two observed in the hindbrain. (F) In another embryo, floorplate labeling appeared in the large gaps between segments of notochord. In this example, a single notochord cell was about 20 μm in diameter and the notochordless gap between it and the next bit of notochord caudal to it was about 80 μm. Labeling of the floorplate in the gap was continuous. When the notochord was completely absent, as in D and E, floorplate labeling was present but discontinuous. In this example, the measurements for the lengths of the rostral-most seven segments of floorplate labeling were 25, 45, 76.5, 83, 51, 52 and 47 μm. The lengths of the gaps between these labeled segments were 23, 18, 23, 13, 19 and 29 μm. At this stage, the average floorplate cell width measured in histological sections was around 5 μm. (I) Even in the complete absence of any notochord labeling, eye vesicles form. (J) In transverse sections of a normal embryo, at the rostral trunk level, staining was restricted to the notochord and the floorplate. The early shield-deletion embryos lacked the notochord in the head and trunk regions (K), but the labeling of the ventral neural axis at the position of the floorplate was clear. The somitic mesoderm (s) was fused medially under the neural tube. Abbreviations: e, eye; fp-l, floorplate labeling; n-l, notochord labeling; nc-l, notochord cell labeling; ov, otic vesicle; s, somitic mesoderm. Scale bar: A, 200 μm; B, 100 μm; C, 50 μm; D, 200 μm; E, 200 μm; F, 50 μm; G, 200 μm; H, 200 μm; I, 50 μm; J-K, 50 μm. Stage 15 hours.

embryos (see Stern, 1993), the node in mouse embryos (Beddington, 1994) and the embryonic shield in teleostean fish embryos (Oppenheimer, 1936b) all possess this 'organizer' activity.

By grafting an embryonic shield into the ventral germ ring of same-stage recipients, we show that the embryonic shield region of the zebrafish has the capacity to induce the formation of a secondary axis. In this way, our results confirm and lend support to the notion that the teleostean shield is a 'center of organization' like the amphibian dorsal lip and the node in chicken (see Stern, 1993) and mouse (Beddington, 1994) embryos. However, the tissue contributions made by the zebrafish shield is different from what had been reported in comparable grafting experiments using the *Xenopus* dorsal lip (Smith and Slack, 1983). The zebrafish shield consistently contributed neural tissues in the ectopic axis, whereas the *Xenopus* dorsal lip did not. This was surprising considering the reported similarities between the zebrafish and amphibian embryos (Kimmel et al., 1990; Warga and Kimmel, 1990). However, the ability of the zebrafish shield to make neural tissues is not atypical of vertebrates, as it is shared by other teleostean embryos (Oppenheimer, 1936b) and has been reported for the chicken (Sulik et al., 1994; Inagaki and Schoenwolf, 1993) and the mouse (Beddington, 1994). An explanation for this difference between the *Xenopus* dorsal lip and similar organizing centers in the fish, chicken and mouse may be found by comparing the fate maps of these organisms. In amphibians, at the onset of gastrulation, the prospective mesodermal and ectodermal domains are largely separate (Vogt, 1929; Keller, 1975, 1976). Because of this, it is possible to excise and transplant the dorsal lip without including presumptive neurectoderm. In contrast, the zebrafish, chicken and mouse embryos all have neural progenitors within their organizers. The mesodermal and neural progenitors are intermingled within the zebrafish shield region (Shih and Fraser, 1995) and both the chicken and mouse nodes contain cells that are common progenitors for mesodermal and neural lineages (Lawson et al., 1991; Lawson and Pedersen, 1992; Selleck and Stern, 1991; Tam and Beddington, 1992; Smith et al., 1994). Thus, it would have been surprising had the zebrafish embryonic shield graft not contributed to ectopic neural tissues.

A comparison of fate maps alone does not explain why the notochord is consistently shorter in the ectopic axis and why the graft makes a larger contribution to the ectopic neural axis than its normal fate would suggest. Unlike homotopic replacements, in which the shield contributes to the ventral neuraxis

from the hindbrain level to that of the anus, in ectopic transplantations, the graft gives rise to more than half of the shorter ectopic neural tube (in cross-sectional view). Oppenheimer made similar observations concerning the degree of neural contributions made by heterotopic shield grafts in her experiments. She found, in *Fundulus*, that grafted cells were sometimes "transformed to forebrain, some formed notochord..." (Oppenheimer, 1936b p422); in *Perca*, she observed that the "dorsal lip" graft was sometimes "completely transformed to brain-like tissue in the head of the host..." (ibid., p423). Taken together, these observations might indicate that prospective notochord cells can convert to a neural fate when challenged in heterotopic grafts in some teleostean species, including zebrafish. Fate conversions have been noted during gastrula stages in *Xenopus*: Small grafts from within the notochord region consistently contribute to somites when transplanted to the ventral marginal zone (Shih and Keller, 1992; Shih, 1991) and prospective epidermal and somitic cells can be induced to take on notochord behavior and fate (Domingo and Keller, 1995). A simple prediction from this 'fate-conversion proposal' would be that the apportionment of neural-versus-notochordal fates in the shield region is a dynamic process at the early-shield stage and that increasing or decreasing the quantity of shield-region tissues should produce clear cases of reapportionment.

In an earlier paper (Shih and Fraser, 1995), we speculated on the relationship between the neural and mesodermal progenitors within the zebrafish shield region. We proposed that the intermingled arrangement of progenitor cells might provide an opportunity for neural induction by the early-shield stage. Such early inductive interactions could take place largely, if not entirely, within the plane of the blastoderm, prior to germ-ring formation. (For planar induction see Keller et al., 1992; Doniach, 1992; Ruiz i Altaba, 1992.) The results of our shield-deletion experiment represents a test of this proposal. If, on one hand, neural induction is already underway by the early shield stage in the zebrafish, then the excision of the organizer and its progeny should produce an embryo displaying some degree of neural development and patterning. If, on the other hand, cell-fate specification begins only after the onset of germ ring formation (Ho and Kimmel, 1993), then deleting the shield should lead to a failure of neural development. The results are consistent with the first possibility. Shield deletion produced embryos that were, in some cases, completely without notochord cells, but nevertheless had remarkably well-patterned nervous systems. Similar experiments involving the deletion of either a portion or all of the embryonic shield in other teleosteans also produced embryos without chorda but that had patterned neural structures (Luther, 1935; Oppenheimer, 1936b; Sumner, 1904; Devillers, 1948a,b). The one exception to this general trend in teleosts was reported by Trinkaus (Trinkaus, 1951), in which no embryo formed following shield excision in the *Fundulus heteroclitus* gastrula, although pigment cells (possibly neural crest cells) did form. This observation was recently reproduced as a minority case along side the majority result reported by Oppenheimer (Shih and Trinkaus unpublished results). These results suggest that neural induction may begin early in teleostean embryos, even before germ ring formation. If this 'early' neural induction is a consequence of the intermingling of tissue progenitors within a center of organization, then one might expect a similarly 'early' induction event in the chicken and mouse embryos, but not in amphibians. Results consistent with this proposal may be found in experiments in chicken embryos where the notochord was reduced to a very few cells following node excision, yet a seemingly well-developed neuraxis formed (Grabwoski, 1956).

Recently, it was reported that knocking out *HNF3β*, a factor important for notochord formation, produced mice that were able to form a remarkably well-patterned nervous system in the complete absence of a notochord (Ang and Rossant, 1994; Weinstein et al., 1994). As neither the notochord nor the node form in the absence of *HNF3β*, neither structure could have induced and patterned the observed neuraxis. These results suggest an alternate explanation for the shield-deletion phenotype presented here: it may be that tissues other than those originating in the shield region can compensate for the loss of the organizer's inductive influence. (See also Ang and Rossant, 1994 and Weinstein et al., 1994 for additional discussion on this point). There is evidence in the zebrafish to support this second explanation. Characterization of the floating head mutation (*flh*) suggests that at least notochord formation per se is not essential for neural induction and patterning (Talbot et al., 1995). Even in *Xenopus*, ultraviolet irradiation of the uncleaved fertilized egg can produce notochord-less embryos without completely eliminating neural structures (Clarke et al., 1991). Although such arguments are compelling, it remains to be shown if, at onset of zebrafish germ ring formation, tissues other than those represented in the organizer can induce and pattern the nervous system to such a remarkable degree. Moreover, it is not known whether these tissues, if they exist, normally participate in neural induction during development. We have performed preliminary experiments to address the first question, by grafting tissues other than those within the shield region to determine if they can also organize ectopic axis formation. Early results show that grafting germ ring tissues located immediately lateral to the embryonic shield region into the ventral germ-ring does not result in the formation of an ectopic axis (unpublished observation). In addition, similar experiments transplanting prechordal mesoderm failed to produce a secondary axis with eye(s) or flanking somitic arrays (unpublished observation).

In conclusion, we propose that the zebrafish and perhaps all vertebrate embryos have some capacity to regulate for the physical loss of the organizer by compensating for its activity. There are many possibilities for how this regulation may be achieved. This regulation may be driven by an up-regulation of inducing capacity in some residual organizer cells left over in the embryo after the bulk of the organizer is excised. Alternately, cells that normally do not have organizing capacity may come to express the ability to induce and pattern the neuraxis following organizer deletion. Lastly, it may be that normal neural induction and patterning is influenced by interactions that include, but are not limited to, organizer activity. These proposals each suggest experiments that should better characterize the inducing capacity of the vertebrate organizer at the molecular, cellular and tissue levels.

The authors express heart-felt appreciation to all those who supported our research through its difficult early years. We would like to especially thank Drs J. P. Trinkaus, Ray Keller, Eric Davidson, Jane Oppenheimer and William Ballard for their encouragement and

insights. Moreover, we thank Dr Katherine Woo for her critical reading of the manuscript and many valuable discussions. We wish to express our gratitude to Woods Hole Marine Biology Laboratory, where these experiments were first performed in the summer of 1992, in the middle of the great *Swoopenella* outbreak. Finally, we would also like to express our thanks to Dian De Sha for her help in editing and re-editing the manuscript. This research was supported by the NIH and a NIH Post-Doctoral Training Fellowship #5T32 HD07257.

REFERENCES

Ang, S.-L. and Rossant, J. (1994). *HNF3ß* is essential for node and notochord formation in mouse development. *Cell* **78**, 561-574.

Bautzmann, H. (1926). Experimentelle Untersuchungen zur Abgrenzung des Organisationszentrums bei *Triton taeniatus*, mit einem Anhang: Uber Induktion durch Blastulamaterial. *Wilhelm Roux Arch. EntwMech. Org.* **108**, 283-321.

Beddington, R. S. P. (1994). Induction of a second neural axis by the mouse node. *Development* **120**, 613-620.

Clarke, J. D. W., Holder, N., Soffe, S. R. and Strome-Methisen, J. (1991). Neuroanatomical and functional analysis of neural tube formation in notochordless *Xenopus* embryos; laterality of the ventral spinal cord is lost. *Development* **112**, 499-516.

Devillers, M. C. (1948a). Méchanique gastruléenne du l'œuf de Truite (*Salmo*). *C. R. Acad. Sci. (Paris)* **226**, 1310-1312.

Devillers, M. C. (1948b). Suppression du matérial chordal dans la gastrula de Truite. *C. R. Acad. Sci. (Paris)* **227**, 1411-1413.

Domingo, C. and Keller, R. E. (1995) Induction of notochord cell intercalation behavior and differentiation by progressive signals in the gastrula of *Xenopus laevis*. *Development* **121**, 3311-3321

Doniach, T. (1992). Planar induction of Anteroposterior Pattern in the Central Nervous System of *Xenopus laevis*. *Science* **257**, 542-545.

Grabowski, C. T. (1956). The effects of the excision of Hensen's node on the early development of the chick embryo. *J. Exp. Zool.* **133**, 301-343.

Ho, R. K. (1992). Axis formation in the embryo of the zebrafish, *Brachydanio rerio*. *Seminars in Developmental Biology* **3**, 53-64.

Ho, R. K. and Kimmel, C. B. (1993). Commitment of cell fate in the early zebrafish embryo. *Science* **261**, 109-11.

Inagaki, T. and Schoenwolf, G. C. (1993). Axis development in avian embryos: the ability of Hensen's node to self-differentiate, as analyzed with heterochronic grafting experiments. *Anat. Embryol.* **188**, 1-11.

Keller, R. (1991). Early embryonic development in *Xenopus laevis*. In *Methods in Cell Biology* vol. 36 (ed. B. K. Kay and H. B. Peng), pp. 62-113. San Diego: Academic Press Inc.

Keller, R. E. (1975). Vital dye mapping of the gastrula and neurula of *Xenopus laevis*. I. Prospective areas and morphogenetic movements of the superficial layer. *Dev. Biol.* **42**, 222-241.

Keller, R. E. (1976). Vital dye mapping of the gastrula and neurula of *Xenopus laevis*. II. Prospective areas and morphogenetic movements of the deep layers. *Dev. Biol.* **51**, 118-137.

Keller, R. E., Shih, J., Sater, A. and Moreno, C. (1992). Planar induction of convergence and extension of the neural plate by the organizer of *Xenopus*. *Dev. Dynamics* **193**, 218-234.

Kimmel, C. B., Warga, R. M. and Schilling, T. F. (1990). Origin and organization of the zebrafish fate map. *Development* **108**, 581-594.

Kimmel, C. B., Ballard, W. W., Kimmel, S. R., Ullmann, B. and Schilling, T. F. (1995). Stages of Embryonic Development of the Zebrafish. *Dev. Dynamics* **203**, 253-310.

Klymkowsky, M. W. and Hanken, J. (1991). Early embryonic development in *Xenopus laevis*. In *Methods in Cell Biology* vol. 36 (ed. B. K. Kay and H. B. Peng), pp. 419-441. San Diego: Academic Press Inc.

Lawson, K. A., Meneses, J. J. and Pedersen, R. A. (1991). Clonal analysis of epiblast fate during germ layer formation in the mouse embryo. *Development* **113**, 891-911.

Lawson, K. A. and Pedersen, R. A. (1992). Clonal analysis of cell fate during gastrulation and early neurulation in the mouse. In *Postimplantation Development in the Mouse.* vol. 165 (ed. Wiley and Chichester), pp. 3-26.

Luther, W. H. (1935). Entwicklungsphysiologische Untersuchungen am Forellenkeim: Die Rolle des Organisationszentrums bei der Entstehung der Embryonalanlage. *Biol. Zentralbl.* **Bd. 55**, 114-137.

Oppenheimer, J. M. (1936a). Structures developed in amphibians by implantation of living fish organizer. *Proc. Soc. Exp. Biol. Med.* **34**, 461-463.

Oppenheimer, J. M. (1936b). Transplantation experiments on developing teleosts (*Fundulus* and *Perca*). *J. Exp. Zool.* **72**, 409-437.

Ruiz i Altaba, A. (1992). Planar and vertical signals in the induction and patterning of the *Xenopus* nervous system. *Development* **116**, 67-80.

Selleck, M. A. J. and Stern, C. D. (1991). Fate mapping and cell lineage analysis of Hensen's node in the chick embryo. *Development* **112**, 615-626.

Shih, J. (1991). Some aspects of the organization and polarity of the dorsal marginal zone (DMZ) in *Xenopus laevis* gastrula: tissue interactions, motility, and pattern. Ph. D. in Zoology, University of California at Berkeley.

Shih, J. and Fraser, S. E. (1995). The distribution of tissue progenitors within the shield region of the zebrafish gastrula. *Development* **121**, 2755-2765.

Shih, J. and Keller, R. E. (1992). The epithelium of the dorsal marginal zone of *Xenopus* has organizer properties. *Development* **116**, 887-899.

Smith, J. C. and Slack J. M. W. (1983). Dorsalization and neural induction : properties of the organizer in *Xenopus laevis*. *J. Embryol. Exp. Morph.* **78**, 299-317.

Smith, J. L., Gesteland, K. M. and Schoenwolf, G. C. (1994). Prospective fate map of the mouse primitive streak at 7.5 days of gestation. *Dev. Dynamics* **201**, 279-289.

Spemann, H. and Mangold, H. (1924). Induction of embryonic primordia by implantation of organizers from different species. In *Foundations of Experimental Embryology* (ed. B. H. Willier and J. M. Oppenheimer), pp. 144-184. Englewood Cliffs, N. J.: Prentice-Hall Inc.

Spemann, H. (1938). *Embryonic Development and Induction.* New York: Yale University Press.

Stern, C. D. (1993). *Essential developmental biology: a practical approach.* (ed. C. D. Stern and P. W. H. Holland). Oxford, New York: Oxford University Press.

Sulik, K., Denhart, D. B., Inagaki, T., Carson, J. L., Vrablic, T., Gesteland, K. and Schoenwolf, G. C. (1994). Morphogenesis of the murine node and notochordal plate. *Dev. Dynamics* **201**, 260-278.

Sumner, F. B. (1904). A study of early fish development. Experimental and Morphological. *Wilhelm Roux Arch. EntwMech. Organ* **17**, 92-149.

Talbot, W. S., Trevarrow, B., Halpern, M. E., Melby, A. E., Farr, G., Postlethwait, J. H., Jowett, T., Kimmel, C. B. and Kimelman, D. (1995). A homeobox essential for zebrafish notochord development. *Nature* **378**, 150-157.

Tam, P. P. L. and Beddington, R. S. P. (1992). Establishment and organization of germ layers in the gastrulating mouse embryo. In *Postimplantation Development in the Mouse.* vol. 165 (ed. Wiley and Chichester), pp. 27-49.

Trinkaus, J. P. (1951). Analysis of blastoderm expansion in epiboly of the egg of *Fundulus heteroclitus*. *Anat. Records* **111**, 550-551.

Vogt, W. (1929). Gestaltanalyse am Amphibienkein mit örtlicher Vitalfarbung. II. Teil. Gastrulation und Mesodermbildung bei Urodelen und Anuren. *Wilhelm Roux Arch. EntwMech. Org.* **120**, 384-706.

Warga, R. M. and Kimmel, C. B. (1990). Cell movements during epiboly and gastrulation in zebrafish.. *Development* **108**, 569-80.

Weinstein, D. C., Ruiz i Altaba, A., Chen, W. S., Hoodless, P., Prezioso, V. R., Jessell, T. M. and Darnell, J. E. J. (1994). The winged-helix transcription factor *HNF3ß* is required for notochord development in the mouse embryo. *Cell* **78**, 575-588.

Westerfield, M. (1994). *The Zebrafish Book: A Guide for the Laboratory Use of Zebrafish (Brachydanio rerio)*. Eugene: University of Oregon Press.

(Accepted 27 January 1996)